ADVANCES IN ATMOSPHERIC SCIENCES, VOL. 29, NO. 6, 2012, 1238–1248

Seasonal Evolution of Dominant Modes in South Pacific SST and Relationship with ENSO

LI Gang*[1] (李 刚), LI Chongyin[1,2] (李崇银), TAN Yanke[1] (谭言科), and BAI Tao[1,3] (白 涛)

[1]*Institute of Meteorology and Oceanography, PLA University of Science and Technology, Nanjing* 211101

[2]*State Key Laboratory of Numerical Modeling for Atmospheric Sciences and Geophysical Fluid Dynamics, Institute of Atmospheric Physics, Chinese Academy of Sciences, Beijing* 100029

[3]*No.* 94162 *Troops of PLA, Xi'an* 710614

(Received 12 October 2011; revised 14 February 2012)

ABSTRACT

A season-reliant empirical orthogonal function (S-EOF) analysis was applied to the seasonal mean SST anomalies (SSTAs) based on the HadISST1 dataset with linear trend removed at every grid point in the South Pacific (60.5°–19.5°S, 139.5°E–60.5°W) during the period 1979–2009. The spatiotemporal characteristics of the dominant modes and their relationships with ENSO were analyzed. The results show that there are two seasonally evolving dominant modes of SSTAs in the South Pacific with interannual and interdecadal variations; they account for nearly 40% of the total variance. Although the seasonal evolution of spatial patterns of the first S-EOF mode (S-EOF1) did not show remarkable propagation, it decays with season remarkably. The second S-EOF mode (S-EOF2) showed significant seasonal evolution and intensified with season, with distinct characteristics of eastward propagation of the negative SSTAs in southern New Zealand and positive SSTAs southeast of Australia. Both of these two modes have significant relationships with ENSO. These two modes correspond to the post-ENSO and ENSO turnabout years, respectively. The S-EOF1 mode associated with the decay of the eastern Pacific (EP) and the central Pacific (CP) types of ENSO exhibited a more significant relationship with the EP/CP type of El Niño than that with the EP/CP type of La Niña. The S-EOF2 mode contacted with the EP type of El Niño changing into the EP/CP type of La Niña showed a more significant connection with the EP/CP type of La Niña.

Key words: South Pacific, sea surface temperature anomalies, season-reliant empirical orthogonal function (S-EOF), El Niño-Southern Oscillation (ENSO)

Citation: Li, G., C. Y. Li, Y. K. Tan, and T. Bai, 2012: Seasonal evolution of dominant modes in South Pacific SST and relationship with ENSO. *Adv. Atmos. Sci.*, **29**(6), 1238–1248, doi: 10.1007/s00376-012-1191-z.

1. Introduction

The Southern Hemisphere oceans comprise a vast domain, and they play important roles in the global climate system. Many studies have investigated the SST variations in these region and their impacts on the global climate, including the South Indian Ocean (Behera and Yamagata, 2001; Jia and Li, 2005; Yan et al., 2009), the South Atlantic Ocean (Venegas et al., 1997, 1998; Weijer et al., 2002; Nnamchi and Li, 2011), the southeastern Pacific (Shaffer et al., 2000; Falvey and Garreaud, 2009), and the southwestern Pacific (Holbrook and Bindoff, 1999; Holbrook et al., 2005). The SST anomalies in these regions exhibit significant interannual and decadal variations and have close relationships with El Niño-Southern Oscillation (ENSO).

The South Pacific region covers nearly half of the Southern Hemisphere oceans, spanning from the equator to 60°S and from ∼140°E to 70°W. However, relative to the North Pacific, fewer ocean observations take place in the South Pacific because of not only its inhospitable environment but also the paucity of observation stations (Reynolds and Smith, 1994; Linsley et al., 2000; Smith et al., 2008). Therefore, the

*Corresponding author: LI Gang, ligang.1983@163.com

ocean reanalyzed datasets based on assimilation models and interpolated methods have to be used to study South Pacific ocean–atmosphere interactions. In fact, the lack of high-quality sea temperature data hampers the study of the South Pacific to some extent.

Despite the lack of high-quality ocean observations in the South Pacific, ocean temperature datasets based on the satellite are available dating to the late 1970s; they provide a basis for study the ocean–atmosphere interactions in the South Pacific. Many studies have been conducted on the South Pacific; they are mainly focused on the sea temperature (surface and subsurface temperatures) variability on the interannual and decadal time scales (Wang and Liu, 2000; Luo and Yamagata, 2001; Giese et al., 2002; Kidson and Renwick, 2002; Luo et al., 2003; Yu and Boer, 2004; Wang et al., 2007; Yang et al., 2007; Shakun and Shaman, 2009) and its impact on global climate variability (Barros and Silvestri, 2002; Hsu and Chen, 2011). These studies have not only suggested that both the surface and subsurface temperature anomalies in South Pacific can propagate to the tropical Pacific, but they have also reported that ENSO has an important impact on the South Pacific SST anomalies. In addition, the SST anomalies in the South Pacific feature significant decadal and interdecadal variations.

However, what are the dominant modes of SST anomalies in the entire South Pacific on an interannual time scale? The answer to this question is not straightforward because the SST variations in this region seem to have a closer association with the evolution of ENSO than in the North Pacific (Wang et al., 2003a, b; Shakun and Shaman, 2009). When conventional EOF analysis and singular value decomposition (SVD) analysis are applied to the SST anomalies in the South Pacific, the first mode obtained has a close relationship with ENSO in the mature phase, which reflects the response of SST variations in the South Pacific to ENSO. Previous studies have applied EOF analysis to either boreal summer SST anomalies or boreal winter SST anomalies in the South Pacific (Hsu and Chen, 2011; Li et al., 2011). The resultant modes of SST anomalies are closely associated with the evolution of ENSO. Therefore, the SST anomalies in the South Pacific may show significant seasonal evolution characteristics. In this study, we used a season-reliant EOF (S-EOF) analysis to extract the major modes of SST anomalies in the South Pacific.

The goals of this study were to identify the spatiotemporal characteristic of the leading seasonally evolving modes of the South Pacific and to determine their relationships with ENSO during recent decades (i.e., after the 1976/1977 climate shift).

This paper is organized as follows: Section 2 briefly describes the datasets and analysis methods used in present study. In section 3, we identify the main seasonally evolving modes of the South Pacific. Section 4 describes the relationships between these patterns of variability and ENSO. The conclusions and some discussions are summarized in section 5.

2. Data and analysis methods

2.1 *Data*

The principal data used in this study were sea surface temperature (SST) data (horizontal resolution $1^\circ\times1^\circ$) from the Hadley Centre Sea Ice and Sea Surface Temperature datasets (HadISST1) of the UK Meteorological Office (Rayner et al., 2003). Although this dataset is available from 1870 to the present, our analyses only considered decades following the 1976/1977 climate shift. We chose to analyze the period 1979–2009.

Anomalous quantities were computed by removing the monthly mean climatology and the linear trend based on a linear least squares fit. Given that array $y(n)$ is the SST data and array $x(n)$ is the time index of SST data $y(n)$, the linear trend was fitted as $y(n) = a\times x(n)+b$. Then we removed this linear trend from the SST.

We used the Niño3.4 index (available online at http://www.esrl.noaa.gov/psd/gcos_wgsp/Timeseries/) as an indicator of the ENSO variability. The Niño3.4 index was calculated from the HadISST1 using the averaged SST over the study region (5°S–5°N, 170°E–120°W).

2.2 *Analysis methods*

Season-reliant empirical orthogonal function (S-EOF) was the primary method used in this study. Although conventional EOF analysis can depict the spatiotemporal variations of a physical field, it cannot produce coherently seasonal evolution patterns. S-EOF analysis is similar to the extended EOF (EEOF; Weare and Nasstrom, 1982) analysis to some extent. The idea of S-EOF has been discussed in detail by Wang and An (2005). In this study we applied the S-EOF analysis to SST anomalies in a seasonal sequence beginning from the winter of a year denoted as D(−1)JF(0) to the following fall, denoted as SON(0). We treated the anomalies for D(−1)JF(0), MAM(0), JJA(0), and SON(0) as a "yearly block", where −1 denotes the year before year 0. When the conventional EOF analysis was conducted, the yearly block was divided into four consecutive seasonal anomalies to obtain a seasonally evolving mode of the SST anomalies. In our analysis, we also used the Morlet wavelet to identify the periodicity of the seasonally evolving modes (Tor-

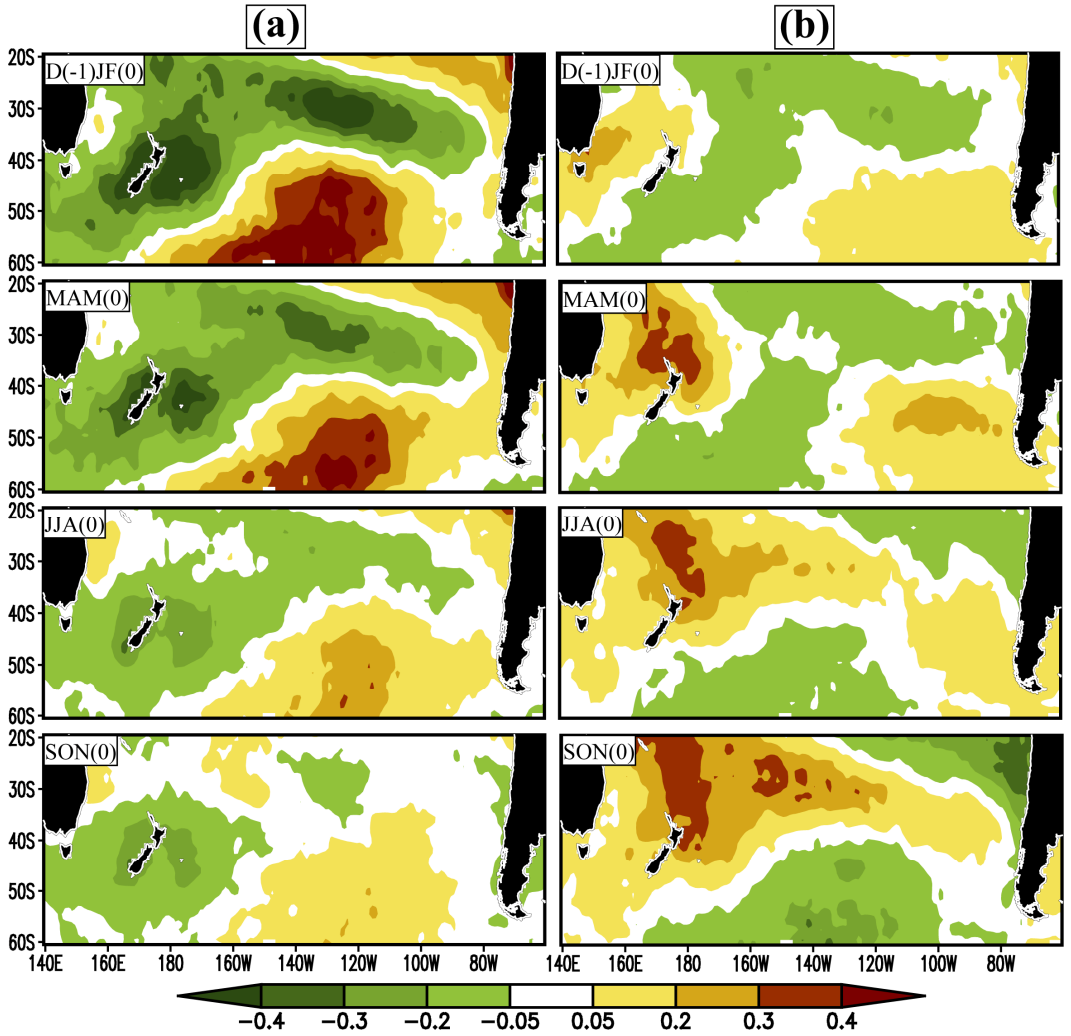

Fig. 1. (a) Seasonally evolving spatial patterns of S-EOF1 mode derived from the HadISST1 SST anomalies over the South Pacific during the period 1979–2009 (°C). (b) The same as in panel (a), but for S-EOF2 mode.

rence and Compo, 1998). In addition, we used regression and correlation methods; statistical significance of correlation coefficients was assessed using the Student's t-test.

We defined the South Pacific to be the area between 60.5°–19.5°S and 139.5°E–60.5°W. The choice of 19.5°S as the northern boundary excluded the impact of the farthest ENSO.

3. Dominant seasonally evolving SST anomaly patterns

We first applied S-EOF analysis to identify the leading modes of SST anomalies in the South Pacific. The leading two modes accounted for 25.7% and 14.1% of the total variance, respectively. According to the rule of North et al. (1982), we found that these two modes were well distinguished from each other and from the remaining modes. Therefore, these two modes are considered statistically distinguishable and significant. We explored the distinctive seasonal evolution characteristics of these two dominant modes, and we report our findings the following discussion.

Figure 1a shows the seasonally evolving spatial patterns of S-EOF1 mode. Notably, the patterns are derived using regression of the South Pacific SST anomalies from boreal winter [D(−1)JF (0)] to fall [SON(0)], with the first normalized principal component (PC1). In general, we found that S-EOF1 mode is characterized by a tripolar configuration, with a positive SST anomalies centered in the high latitudes of the South Pacific region (60°–50°S, 160°–120°W), surrounded by two negative SST anomalies centered over eastern New Zealand and the mid-latitude South Pacific region (35°–25°S, 140°–100°W), respectively. The strongest tripolar pattern was observed in D(−1)JF(0); it was

consistent with the SST pattern forced by ENSO (Wang et al., 2007; Shakun and Shaman, 2009). Although the positive SST anomalies of S-EOF1 show a slight eastward shift, the positions of both the positive and negative SST anomalies of S-EOF1 do not show significant seasonal dependence. However, the amplitude of the S-EOF1 mode shows pronounced characteristics of seasonal evolution. In fact, both the positive and negative SST anomalies decayed rapidly from D(−1)JF(0) to SON(0).

Figure 1b presents the seasonally evolving spatial patterns of S-EOF2 mode. The S-EOF1 and S-EOF2 mode are clearly distinguished from each other by their seasonal evolution. In sharp contrast with S-EOF1, S-EOF2 mode features a wavelike pattern from the northwestern to the southeastern Pacific, with positive SST anomalies in southeastern Australia and the southeastern Pacific (60°–40°S, 130°–80°W) and negative SST anomalies over southeastern New Zealand and the mid-latitude South Pacific. In MAM(0), the positive SST anomalies intensify significantly while the negative SST anomalies over the mid-latitude South Pacific begin to decay. Notably, the positive SST anomalies center over the southeastern Australia shift northeastward to the northern New Zealand from D(−1)JF(0) to MAM(0) and then become stationary, but they develop with season remarkably. From MAM(0) to SON(0), both the positive SST anomalies over the northern New Zealand and negative SST anomalies over the southern New Zealand extend eastward and intensify with season. However, the positive SST anomalies over the southeastern South Pacific decay from MAM(0) to SON(0). The eastward propagation of the positive SST anomalies in the eastern Australia is consistent with the results of Kidson and Renwick (2002), who found that large-scale South Pacific SST variations on the interannual time scale are primarily driven by ENSO.

Compared with conventional EOF analysis, S-EOF analysis can depict the seasonal evolution of a physical field. However, the pattern of S-EOF1 mode in D(−1)JF(0) over the South Pacific (Fig. 1a) resembles the pattern obtained from conventional EOF analysis of SST anomalies in D(−1)JF (0), not only using the same dataset (Wang et al., 2007; Shakun and Shaman, 2009; Terray, 2011) but also using different datasets (Li et al., 2011), even though both the time period and the spatial coverage of the data used in the analyses were different. In addition, the pattern of S-EOF2 mode in D(−1)JF(0) (Fig. 1b) also resembles that based on conventional EOF analysis of SST anomalies in D(−1)JF(0), only with the reverse sign (Li et al., 2011). This resemblance indicates that both S-EOF1 and S-EOF2 mode of the South Pacific are stable and credible. Notably, the resemblance can be observed not only between the patterns of S-EOF1 mode in JJA(0) (Fig. 1a) and S-EOF2 mode in D(−1)JF(0) (Fig. 1b) but also between the patterns of S-EOF1 mode in D(−1)JF(0) (Fig. 1a) and S-EOF2 mode in SON(0). This resemblance between S-EOF1 and S-EOF2 mode reveals that both of these modes have a connection with some important signals (e.g., ENSO; Kidson and Renwick, 2002), but with different lead–lag correlations, which are discussed hereafter.

Although the combination of these two dominant S-EOF modes accounted for nearly 40% of the total variance, the fractional variance explained by the two S-EOF modes varied with season and location remarkably. The spatial and seasonal geographic distributions of the fractional variance for these two modes are shown in Fig. 2. For S-EOF1 mode (Fig. 2a), the foremost prominent feature is that the largest fractional variance occurs in D(−1)JF(0) over the mid-latitude South Pacific along 30°S, over the southwestern Pacific that encompasses the New Zealand, and over the high-latitude South Pacific, where the accounted variance exceeds 60%. The second most notable feature in Fig. 2a is that the fractional variance over the three regions decreases gradually from D(−1)JF(0) to SON(0). For S-EOF2 (Fig. 2b), the prominent feature is that the maximum variance appears in SON(0) over the regions that resemble the first mode in D(−1)JF(0), where the fractional variance exceeds 40%. Notably, the fractional variance carried by the second mode over the northern New Zealand and high-latitude South Pacific features a significant eastward propagation and becomes large gradually with season appreciably. We also noted that the regions with the larger variance are associated with significant SST anomalies.

Figure 3 presents the time series of principal components of S-EOF1 (Fig. 3a) and S-EOF2 (Fig. 3b). The black thick line is the normalized 7-year low-pass filtered time series. The first notable feature in Fig. 3 is that both of these modes have not only prominent interannual variations but also significant interdecadal variations. The second feature is that the amplitude of these two principal components decayed rapidly after 2000. The third prominent feature is the reversal of interdecadal variations (the black thick line in Fig. 3) of the two S-EOF modes.

To investigate the periodicities of the two modes in detail, the local wavelet power spectrum analysis based on Morelet wavelet was applied to their principal components. Figure 4 presents the local wavelet power spectrum of the normalized PC1 (Fig. 4a) and PC2 (Fig. 4b). PC1 shows high power in the 3–5.5-year and 2–3- year bands for the periods 1980–1995

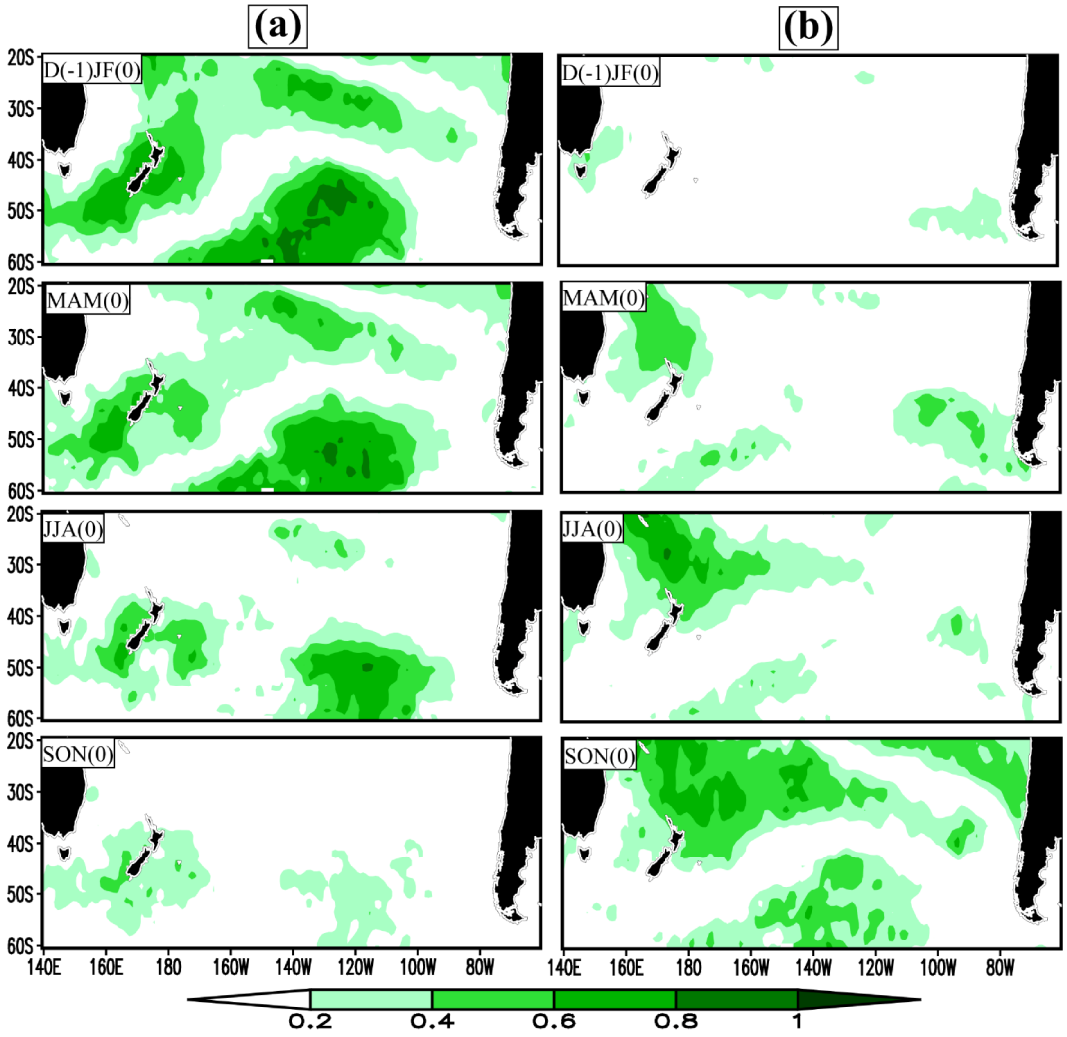

Fig. 2. Fractional variance of the seasonal South Pacific SST anomalies accounted by (a) S-EOF1 and (b) S-EOF2.

and 1995–2000 on the interannual time scale, respectively. However, PC2 has significantly high power in the 2–4-year band for the period 1993–2000 on the interannual time scale. Both of the two modes have pronounced high power in the 8–15-year band on the interdecadal time scale. In addition, the high power of the two modes on the interannual and interdecadal time scales decayed significantly after the year 2000.

4. Relationships between the dominant modes and ENSO

ENSO is the largest well-known signal in the climate system on the interannual time scale. Analysis of the dominant, seasonally evolving SST patterns of the South Pacific show that they may have an association with ENSO. To examine the relationships between the two S-EOF modes and ENSO, we calculated the lead–lag correlations between the PC1 and PC2 and ENSO.

The lead–lag correlations of PC1 with Niño3.4 index are shown in Fig. 5 (blue line). Here the year (−1) denotes that Niño3.4 index leads the PC1 and the year (1) denotes that Niño3.4 index lags the PC1. Notably, the PC1 was positively correlated with the Niño3.4 index from JJA(−1) to MAM(0), with the correlation coefficient passing the threshold of significance in the 95% Student's t-test. The PC1 shows a maximum positive correlation coefficient that exceeds 0.8 (statistically significant at the 95% Student's t-test significance) in D(−1)JF(0). After the correlation coefficient reaches its peak in D(−1)JF(0), the correlation between them decays rapidly and becomes negative (not passing the 5% Student's t-test significance) that persists after SON (0).

The lead–lag correlation between PC2 and the

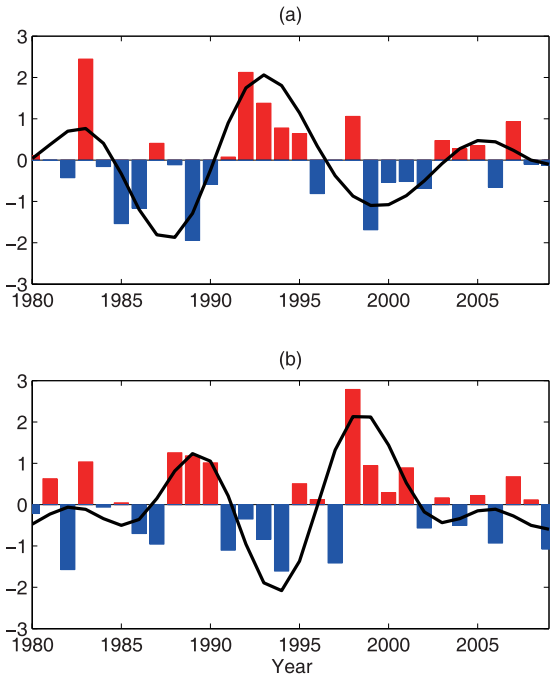

Fig. 3. Normalized principal components of (a) S-EOF1 mode and (b) S-EOF2 mode. The superimposed black thick line is the normalized 7 year low-pass filtered time series.

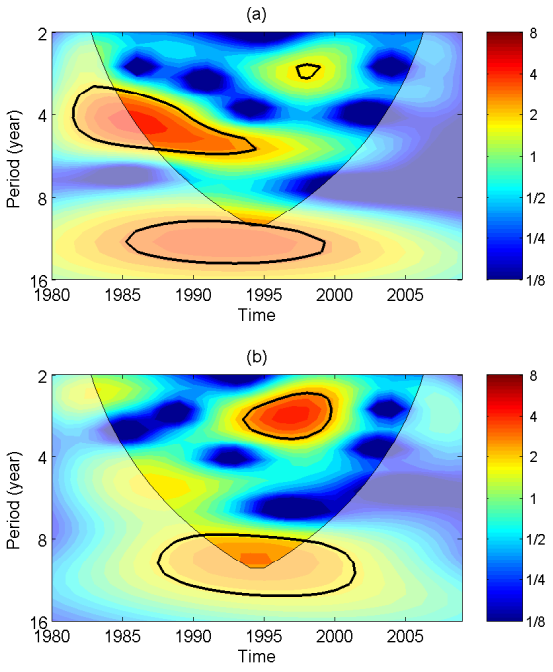

Fig. 4. The local wavelet power spectrum (using the Morlet wavelet) of (a) S-EOF1 and (b) S-EOF2. The thick black contour is the 10% significance level against the red noise. The cone of influence (COI) where edge effects might distort the picture is show as a lighter shade.

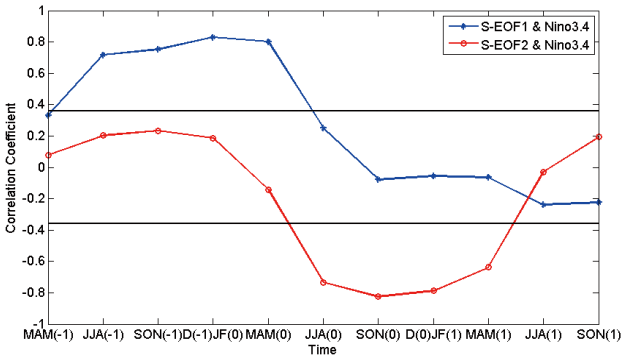

Fig. 5. (a) Lead–lag correlations between the first S-EOF principal component and Niño 3.4 index. (b) The same as in panel (a), but for the second mode. The dashed lines indicate the Student's t-test at 5% significance.

Niño3.4 index is also shown in Fig. 5 (red line). Notably, the correlation is positive and weak (not passing Student's t-test at 5% significance) from MAM(-1) to D(-1)JF(0). However, the correlation becomes negative and rapidly develops from MAM (0) to SON (0). A maximum negative correlation coefficient occurs in SON(0) that passes the threhold of the 5% Student's t-test significance. After the correlation reaches its peak in SON(0), it decays significantly after D(0)JF(1).

As we know, ENSO features significant phase-locking and seasonal cycle behavior, starting in the boreal spring, normally maturing in the boreal winter, and decaying in the next spring (Rasmussen and Carpenter, 1982; Neelin et al., 2000). Based on the correlations between the two modes and ENSO, we can conclude that S-EOF1 mode occurs following the peak of the ENSO, and it may be viewed as responses to ENSO (Shakun and Shaman, 2009). However, S-EOF2 mode is primarily associated with the development of ENSO, and it may impact ENSO (Zhang et al., 2005) and thus may make a significant contribution to ENSO prediction methods.

To further demonstrate the relationship between season-evolving variability of South Pacific SST and ENSO, the spatial patterns of seasonally evolving SST in the tropical Pacific associated with the two S-EOF modes are shown in Figs. 6 and 7, respectively. Here the SST anomalies in the tropical Pacific are regressed with PC1 and PC2. To show the evolution of ENSO, the figures from the last year [year (-1)] to the next year [year (1)] are presented.

Figure 6 shows the seasonal evolution of spatial patterns of tropical Pacific SST anomalies associated with S-EOF1. In D(-2)JF(-1), the positive SST anomalies are primarily located over the central tropical Pacific and extend northeastward to North Amer-

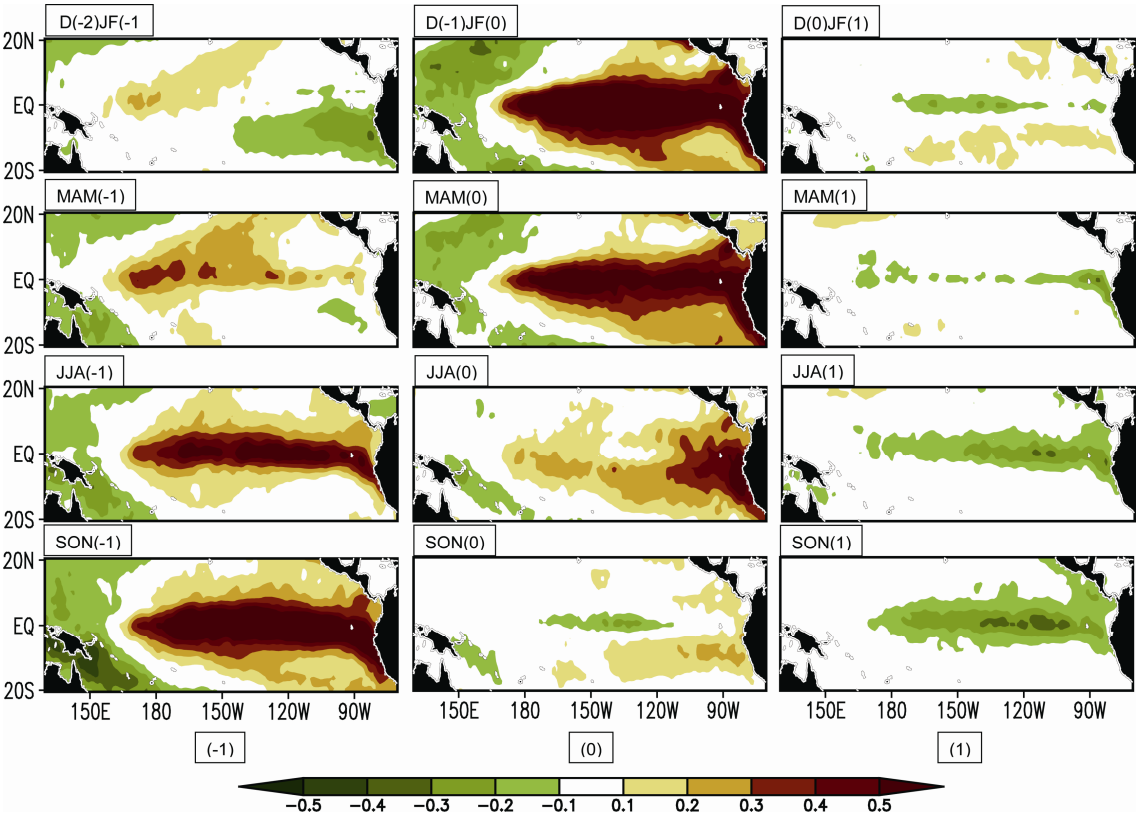

Fig. 6. Seasonally evolving patterns of tropical Pacific SST anomalies regressed with the principal component of S-EOF1 (Units: °C).

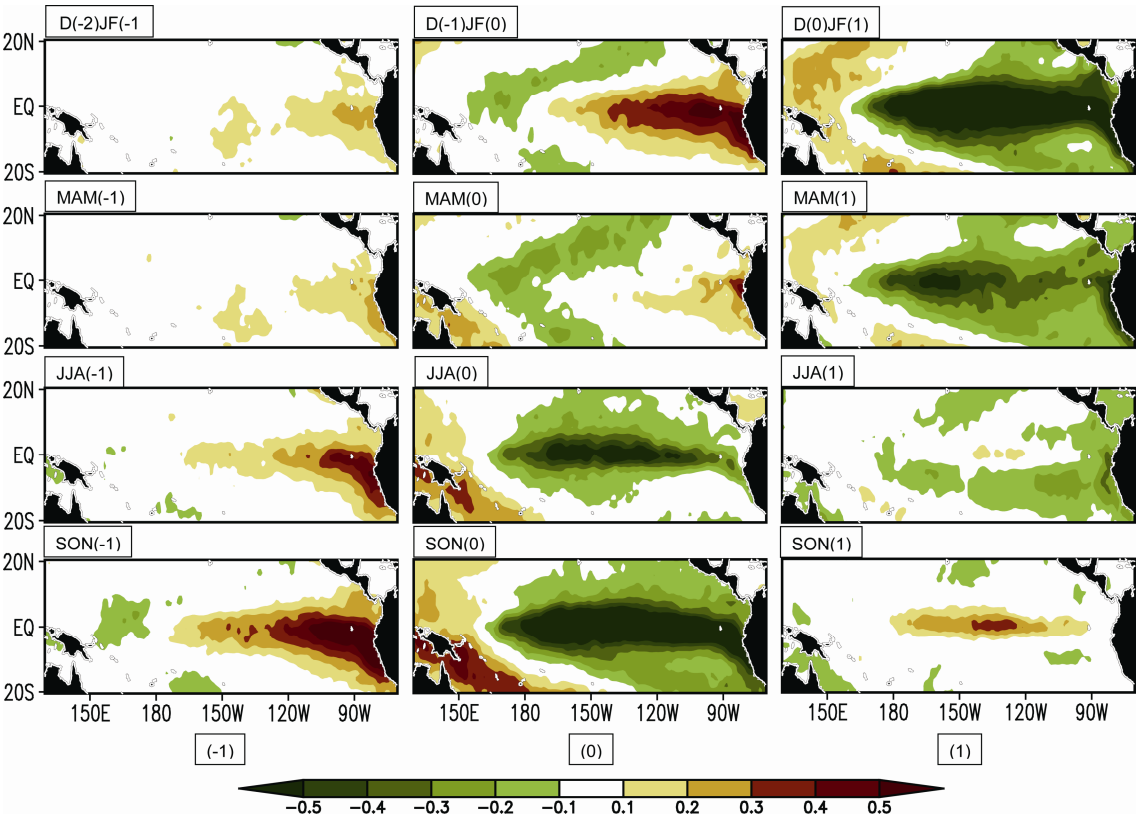

Fig. 7. The same as in Fig. 6, but for S-EOF2 mode.

ica. The negative SST anomalies are mainly found over the southeastern tropical Pacific centered near the western Peruvian coast.

After MAM(−1), the positive SST anomalies in the central tropical Pacific strengthen significantly and propagate eastward along the equator. A weak positive SST anomaly is noticeable in the eastern tropical Pacific and develops rapidly with season. Notably, the amplitude of the eastern tropical Pacific SST anomalies is weaker than that of the SST anomalies in the tropical central Pacific. However, the negative SST anomalies in the tropical southeastern Pacific decay rapidly, and the meridional extent of the negative SST anomalies increases toward North Pacific. This indicates that El Niño develops with the season. The positive SST anomalies in the tropical central-eastern Pacific reach maximum (∼1.1°C) in D(−1)JF(0). The negative SST anomalies are mainly located in the tropical western Pacific. This indicates that El Niño reached the mature phase.

Notably, the positive SST anomalies in the central-eastern tropical Pacific decay rapidly after MAM(0), which indicates that El Niño began to decay. It is necessary to mention that the decay in the central tropical Pacific is more rapid than that in the eastern tropical Pacific. In SON(0), the pattern is nearly a reversal of SST anomalies in D(−2)JF(−1), which indicates that El Niño died out.

From D(0)JF(1) to SON(1), the weak negative SST anomalies in the central tropical Pacific developed with season. The other weak negative SST anomalies in the eastern tropical Pacific emerged near the Peruvian coast, which indicates that a weak La Niña developed and then strengthened with season.

For S-EOF1 mode, ENSO first occurred in the central tropical Pacific and then occurred in the eastern tropical Pacific, which started in the boreal spring and reached the mature phase in boreal winter. In addition, S-EOF1 mode showed a more remarkable correlation with the warm ENSO events than the cold ENSO events. Notably, ENSO-associated S-EOF1 mode had a period of quasi-quadrennial (∼4 years), which resembled the low-frequency (LF) component of ENSO identified by Barnett (1991).

Figure 7 shows the seasonal evolution of spatial patterns of the tropical Pacific SST anomalies associated with S-EOF2. Notably, warming first appears near the Peruvian coast in D(−2)JF(−1) and develops rapidly with season. This warming features a significant westward propagation and reaches its peak (∼0.7°C) in SON(−1), which indicates that El Niño reached mature phase. The warming decays significantly from D(−1)JF(0) to MAM(0), and the negative SST anomalies in the central tropical Pacific develop into the well-known "horseshoe" pattern with season.

In JJA(0), the other negative SST anomalies emerged in the eastern tropical Pacific. The negative SST anomalies in the central-eastern tropical Pacific showed remarkable development from JJA(0) to SON(0), and the positive SST anomalies in the western tropical Pacific also developed rapidly with the season. This indicates the development of La Niña, which reached its peak in D(0)JF(1). Notably, the negative SST anomalies in the central-eastern tropical Pacific begin to decay in MAM(1), while the positive SST anomalies in the western tropical Pacific begin to decay in D(0)JF(1), which indicate the decline of La Niña. In addition, the negative SST anomalies in the central tropical Pacific show a more rapid decay than that in the eastern tropical Pacific.

On the basis of these results, we can infer that the warm phase of ENSO (El Niño) associated with S-EOF2 mode is mainly located in the eastern tropical Pacific. However, the cold phase of ENSO (La Niña) associated with S-EOF2 mode first appears in the central tropical Pacific and then emerges in the eastern tropical Pacific. S-EOF2 mode has a more remarkable relation with La Niña than that with the S-EOF1 mode. In addition, ENSO events normally begin to develop in boreal summer and reach the mature phase in boreal winter. The ENSO events associated with S-EOF2 have a period of quasi-biennial, which is consistent with the quasi-biennial (QB) component of ENSO (Barnett, 1991).

Rasmusson and Wallace (1983) portrayed two kinds of tropical SST variations: (1) The SST is confined to the eastern third of tropical Pacific and spreads westard. (2) The SST firstly appears near the dateline and shows a eastward propagation. Kao and Yu (2009) refer to these two kinds of SST variations as the eastern Pacific (EP) and the central Pacific (CP) types of ENSO, respectively. Yu et al. (2011) further point out that most ENSO events during 1958–2001 are a combination of both the EP and CP types of ENSO, and they refer to these ENSO events as a EP/CP type of ENSO.

Therefore, based on our analyses and on previous studies, we can conclude that S-EOF1 mode has a significant relation with the EP/CP type of ENSO, whereas S-EOF2 mode is associated with not only the EP type of ENSO warm events (EP, El Niño) but also the EP/CP type of ENSO cold events (EP/CP, La Niña).

5. Discussion and conclusion

Based on the season-reliant EOF analysis, we revealed two dominant modes of South Pacific SST

anomalies and their relationships with ENSO in this study. In this section we first summarize the major seasonal-evolution characteristics of the South Pacific SST anomalies and then discuss their relationships with ENSO.

First, we studied the seasonally evolving spatial patterns of the two dominant modes of the South Pacific SSTAs, which accounted for nearly 40% of the total variance. The results of the S-EOF1 featured a tripolar pattern with positive SST anomalies centered over the high-latitude South Pacific region (60°–50°S, 160°–120°W) and two negative SST anomalies centered east of New Zealand and the mid-latitude South Pacific region (35°–25°S, 140°–100°W), respectively. The configuration of the tripolar pattern changed little with season. But the amplitude of this pattern decayed significantly from D(−1)JF(0) to SON(0). S-EOF2 showed a wavelike pattern from northwest to southeast of South Pacific. Both of the positive and negative SST anomalies showed significant eastward propagation, and their amplitude developed remarkably close to season.

Secondly, we noted that the two modes had not only interannual variations but also significant interdecadal variations. S-EOF1 showed high power in the 3–5.5- and 2–3-year band for the period 1980–1995 and 1995–2000 on the interannual time scale, respectively. However, S-EOF2 had significantly high power in the 2–4-year band for the period 1993–2000 on the interannual time scale. Both modes had prominent high power in the 8–15-year band on the interdecadal time scale. In addition, the amplitude of the two principal components decayed rapidly after 2000. The two modes showed reversed variations on the interdecadal time scale.

Finally, we studied the relationships between the two modes and ENSO. The results show that there are significant correlations between the two modes and ENSO. Based on the lead-lag correlations, it is noted that S-EOF1 can be viewed as a response to ENSO and S-EOF2 is primarily associated with the development of ENSO. Moreover, S-EOF2 may make a significant contribution to ENSO prediction. Based on further study, we noted that results of S-EOF1 had a significant relation with EP/CP type of ENSO and the results of S-EOF2 were associated with both the EP type of ENSO warm events (EP-El Niño) and the EP/CP type of ENSO cold events (EP/CP-La Niña).

In this study, some connections between South Pacific SST variability and ENSO were illustrated using data analyses, but our explanations remain somewhat hypothetical. At first, the SST anomalies in both the northern and southern Pacific appear to be a response to ENSO, which is the strongest signal of climate variation; however, the S-EOF1 mode should be mainly a response of SST in the South Pacific to ENSO. ENSO may influence South Pacific SST variations by changing the surface heat fluxes via an "atmospheric bridge" (Alexander et al., 2002; Li et al., 2006). This hypothesis will be further validated using observation analysis and model experiments. Secondly, Fig.1b shows that SST anomalies propagate to the equatorial western Pacific from southeastern Australia and southwestern South America. The propagation of SST anomalies to the equatorial western Pacific is favorable to the occurrence of ENSO, because the SST anomalies in the western tropical Pacific (particularly in the subsurface) and its eastward propagation are a fundamental condition of the occurrence of ENSO (Li and Mu, 2002). Rossby waves play an important role in this propagation (Jacobs et al., 1994; Wang et al., 2007). Therefore, the S-EOF2 is even more closely associated with the occurrence of ENSO than is shown by this study.

In this study we confirmed the relationships between the two S-EOF modes and ENSO. In future work, the EP and CP types of ENSO will be investigated: they may have different impacts on the seasonal evolution of the South Pacific SST, and the influence mechanism remains to be clarified. We will use both the observational analyses and model experiments in these studies. In addition, our analysis is based on data covering 31 years (1979–2009), which may not be long enough to determine the impacts of different types of ENSO on South Pacific SST. Although these results need to be verified using longer datasets, the outputs of coupled climate models may be used to help us understand the results.

Acknowledgements. The authors thank the editor and the anonymous reviewers for their suggestions and comments to significantly improve our manuscript.

REFERENCES

Alexander, M. A., I. Bladé, M. Newman, J. R. Lanzante, N.-C. Lau, and J. D. Scott, 2002: The atmospheric bridge: The influence of ENSO teleconnections on air-sea interaction over the global oceans. *J. Climate*, **15**, 2205–2231.

Barnett, T. P., 1991: The interaction of multiple time scales in the tropical climate system. *J. Climate*, **4**, 269–285.

Barros, V. R., and G. E. Silvestri, 2002: The relationship between sea surface temperature at the subtropical south-central Pacific and precipitation in southeastern South America. *J. Climate,* **15**, 251–267.

Behera, S. K., and T. Yamagata, 2001: Subtropical SST dipole events in the southern Indian Ocean. *Geophys. Res. Lett.*, **28**(2), 327–330.

Falvey, M., and R. D. Garreaud, 2009: Regional cooling in a warming world: Recent temperature trends in the southeast Pacific and along the west coast of subtropical South America (1979–2006). *Geophys. Res. Lett.*, **114**, D04102, doi: 10.1029/2008JD010519.

Giese, B. S., S. C. Urizar, and N. S. Fuckar, 2002: Southern hemisphere origins of 1976 climate shift. *Geophys. Res. Lett.*, **29**(10), 2215–2231.

Holbrook, N. J., and N. L. Bindoff, 1999: Seasonal temperature variability in the upper southwest Pacific Ocean. *J. Phys. Oceanogr.*, **29**, 366–381.

Holbrook, N. J., P. S. L. Chan, and S. A. Venegas, 2005: Oscillatory and propagating modes of temperature variability at the 3–3.5 and 4–4.5 time scales in the upper southwest Pacific Ocean. *J. Climate*, **18**, 719–736.

Hsu, H. H., and Y. L. Chen, 2011: Decadal to bi-decadal rainfall variation in the western Pacific: A footprint of South Pacific decadal variability? *Geophys. Res. Lett.*, **38**, L03703, doi: 10.1029/2010GL046278.

Jacobs, G. A., H. E. Hurlburt, J. C. Kindle, E. J. Metzger, J. L. Mitchell, W. J. Teague, and A. J. Wallcraft, 1994: Decadal-scale trans-Pacific propagation and warming effects on an El Niño anomaly. *Nature*, **370**, 360–363, doi: 10.1126/science.281.5374.240.

Jia, X. L., and C. Y. Li, 2005: Dipole oscillation in the Southern Indian Ocean and its impacts on climate. *Chinese J. Geophys.*, **48**(6), 1238–1249. (in Chinese)

Kao, H. Y., and J. Y. Yu, 2009: Contrasting Eastern-Pacific and Central-Pacific types of El Niño. *J. Climate*, **22**, 615–632.

Kidson, J. W., and J. A. Renwick, 2002: The Southern Hemisphere evolution of ENSO during 1981–99. *J. Climate*, **15**, 847–863.

Li, C., and M. Q. Mu, 2002: A further inquiry on essence of the ENSO cycle. *Advance in Earth Sciences*, **17**(5), 631–638.

Li, C. H., D. Wang, J. Liang, D. Gu, and Y. Liu, 2006: A local positive feedback of the tropical Pacific ocean-atmosphere system on interdecadal timescales. *Chinese Science Bulletin*, **51**(5), 601–606.

Li, G., C. Y. Li, Y. K. Tan, and T. Bai, 2011: Principal modes of the winter SST anomaly in South Pacific and their relationships with ENSO. *Acta Oceanologica Sinica*, **34**(2), 48–56. (in Chinese)

Linsley, B. K., G. M. Wellington, and D. P. Schrag, 2000: Decadal sea surface temperature variability in the subtropical South Pacific from 1726 to 1997 AD. *Science*, **290**(5494), 1145–1148.

Luo, J. J., and T. Yamagata, 2001: Long-term El Niño-Southern Oscillation (ENSO)-like variation with special emphasis on the South Pacific. *J. Geophys. Res.*, **106**(C10), 22211–22227.

Luo, J. J., S. Masson, S. Behera, P. Delecluse, S. Gualdi, A. Navarra, and T. Yamagata, 2003: South Pacific origin of the decadal ENSO-like variation as simulated by a coupled GCM. *Geophys. Res. Lett.*, **30**(24), 2250–2259.

Nnamchi, H. C., and J. P. Li, 2011: Influence of the South Atlantic Ocean Dipole on west African summer precipitation. *J. Climate*, **24**, 1184–1197.

Neelin, J. D., F. F. Jin, and H. H. Syu, 2000: Variations in ENSO phase locking. *J. Climate*, **13**, 2570–2590.

North, G. R., T. L. Bell, R. F. Cahalan, and F. J. Moeng, 1982: Sampling errors in the estimation of empirical orthogonal functions. *Mon. Wea. Rev.*, **110**, 699–706.

Rasmusson, E. M., and T. H. Carpenter, 1982: Variations in tropical sea surface temperature and surface wind fields associated with the Southern Oscillation El Niño. *Mon. Wea. Rev.*, **110**, 354–384.

Rasmusson, E. M., and J. M. Wallace, 1983: Meteorological aspects of the El Niño /Southern Oscillation. *Science*, **222**(4629), 1195–1202.

Rayner, N. A., D. E. Parker, E. B. Horton, C. K. Folland, L. V. Alexander, D. P. Rowell, E. C. Kent, and A. Kaplan, 2003: Global analyses of sea surface temperature, sea ice, and night marine air temperature since the late nineteenth century. *J. Geophys. Res.*, **108**(D14), 4407, doi: 10.1029/2002JD002670.

Reynolds, R. W., and T. M. Smith, 1994: Improved global sea surface temperature analyses using optimum interpolation. *J. Climate*, **7**, 929–948.

Shaffer, G., O. Leth, O. Ulloa, J. Bendtsen, G. Daneri, V. Dellarossa, S. Hormazaball, and P. I. Sehlstedt, 2000: Warming and circulation change in the eastern South Pacific Ocean. *Geophys. Res. Lett.*, **27**(9), 1247–1250.

Shakun, J. D., and J. Shaman, 2009: Tropical origins of North and South Pacific decadal variability. *Geophys. Res. Lett.*, **36**, L19711, doi:10.1029/2009GL040313.

Smith, T. M., R. W. Reynolds, T. C. Peterson, and J. Lawrimore, 2008: Improvements to NOAA's historical merged land-ocean surface temperature analysis (1880–2006). *J. Climate*, **21**, 2283–2296.

Terray, P., 2011: Southern Hemisphere extra-tropical forcing: A new paradigm for El Niño-Southern Oscillation. *Climate Dyn.*, **36**, 2171–2199.

Torrence, C., and G. P. Compo, 1998: A practical guide to wavelet analysis. *Bull. Amer. Meteor. Soc.*, **79**(1), 61–78.

Venegas, S. A., L. A. Mysak, and D. N. Straub, 1997: Atmosphere-ocean coupled variability in the South Atlantic. *J. Climate,* **10**, 2904–2920.

Venegas, S. A., L. A. Mysak, and D. N. Straub, 1998: An interdecadal climate cycle in the South Atlantic and its links to other ocean basins. *J. Geophys. Res.*, **103C**, 24723–24736.

Wang, B., and S. L. An, 2005: A method for detecting season-dependent modes of climate variability: S-EOF analysis. *Geophys. Res. Lett.*, **32**, L15710, doi: 10.1029/2005GL022709.

Wang, D., and Z. Liu, 2000: The pathway of the interdecadal variability in the Pacific Ocean. *Chinese Science Bulletin*, **45**(17), 1555–1561. (in Chinese)

Wang, D., J. Wang, L. Wu, and Z. Liu, 2003a: Regime shifts in the North Pacific simulated by a COADS-driven isopycnal model. *Adv. Atmos. Sci.*, **20**(5), 743–754.

Wang, D., J. Wang, L. Wu, and Z. Liu, 2003b: Relative importance of wind and buoyancy forcing for interdecadal regime shifts in the Pacific Ocean. *Science in China* (*D*), **46**(5), 417–427.

Wang, X., C. Li, and W. Zhou, 2007: Interdecadal mode and its propagating characteristics of SSTA in the South Pacific. *Meteor. Atmos. Phys.*, **98**, 115–124.

Weare, B. C., and J. S. Nasstrom, 1982: Examples of extended empirical orthogonal function analyses. *Mon. Wea. Rev.*, **110**, 481–485.

Weijer, W., W. P. M. De Ruijter, A. Sterl, and S. S. Drijfhout, 2002: Response of the Atlantic overturning circulation to South Atlantic sources of buoyancy. *Global and Planetary Change*, **34**, 293–311.

Yan, H. M., C. Y. Li, and W. Zhou, 2009: Influence of subtropical dipole pattern in southern Indian Ocean on ENSO event. *Chinese J. Geophys.*, **52**(10), 2436–2449. (in Chinese)

Yang, X., Y., R. X. Huang, and D. Wang, 2007: Decadal change of wind stress over the Southern Ocean associated with Antarctic ozone depletion. *J. Climate*, **20**, 3395–3410.

Yu, B., and G. J. Boer, 2004: The role of the western Pacific in decadal variability. *Geophys. Res. Lett.*, **31**, L02204, doi: 10.1029/2003GL018471.

Yu, J. Y., H. Y. Kao, T. Lee, and S. T. Kim, 2011: Subsurface ocean temperature indices for Central-Pacific and Eastern-Pacific types of El Niño and La Niña events. *Theor. Appl. Climatol.*, **103**, 337–344.

Zhang, Q., H. Wang, Y. Zhong, and D. Wang, 2005: An idealized study of the impact of extratropical climate change on El Niño-Southern Oscillation. *Climate Dyn.*, **25**, 869–880.